FOLIA HISTOCHEMICA ET CYTOBIOLOGICA
Vol. 60, No. 2, 2022
pp. 111–124

ORIGINAL PAPER

VIA MEDICA

A chronic moderate methionine administration induced hyperhomocysteinemia associated with cardiovascular disease phenotype in the sand rat *Psammomys obesus*

Fouzia Zerrouk[1], Billel Chaouad[1], Adel Ghoul[1], Naima Chalour[2], Anissa Moulahoum[1], Zineb Khiari[1], Mohamed El Hadi Cherifi[3], Souhila Aouichat[4], Karim Houali[5], Yasmina Benazzoug[1]

[1]Laboratory of Cellular and Molecular Biology, Biochemistry and Remodeling of the Extracellular Matrix, Faculty of Biological Sciences, Houari Boumediene University of Science and Technology (USTHB), Bab Ezzouar, Algiers, Algeria

[2]Laboratory of Physiology of Organisms, Faculty of Biological Sciences, Houari Boumediene University of Science and Technology (USTHB), Bab Ezzouar, Algiers, Algeria

[3]Central Laboratory of Biology, EPH Bologhine Ibn Ziri, Algiers, Algeria

[4]Laboratory of Physiology of Organisms, Team of Cellular and Molecular Physiopathology, Faculty of Biological Sciences, Houari Boumediene University of Science and Technology (USTHB), Bab Ezzouar, Algiers, Algeria

[5]Laboratory of analytic biochemistry research and biotechnology, Faculty of Biological Sciences and Agronomic Sciences, Mouloud Mammeri University, Tizi-Ouzou, Algeria

Abstract

Introduction. Cardiovascular diseases were defined as coronary artery, cerebrovascular, or peripheral arterial disease. Hyperhomocysteinemia (Hhcy) is an independent risk factor of cardiovascular diseases, including atherosclerosis. Our previous studies demonstrated the involvement of Hhcy in cardiovascular remodeling in the sand rat *Psammomys obesus.*

Material and methods. An experimental Hhcy was induced, in the sand rat *Psammomys obesus*, by a daily intraperitoneal injection of 70 mg/kg of methionine for a total duration of 6 months. The impact of Hhcy on the cellular and matrix structures of the heart, aorta and liver was analyzed using histological techniques. Additionally we treated primary cultures of aortic smooth muscle cells (SMCs) with high concentration of methionine to investigate the effects of methionine at the cellular level.

Results. A moderate Hhcy induced a significant increase in the extracellular matrix components particularly collagens which accumulated in the interstitial and perivascular spaces in the studied organs indicating a developing fibrosis. A liver steatosis was also observed following methionine treatment. Further analysis of the aorta showed that Hhcy also induced vascular alterations including SMCs reorientation and proliferation associated with aneurysm formation.

Conclusions. Our results show for the first time that Hhcy can induce a cardiovascular and liver diseases phenotype in *Psammomys obesus*, a species previously shown to be a good model for the studies of diabetes and other metabolism-related pathologies. *(Folia Histochemica et Cytobiologica 2022, Vol. 60, No. 2, 111–124)*

Correspondence address: Fouzia Zerrouk
Biochemistry and Remodeling of the Extracellular Matrix, Laboratory of Cellular and Molecular Biology, Faculty of Biological Sciences, Houari Boumediene University of Science and Technology (USTHB), Bab Ezzouar, El Alia, 16111, Algiers, Algeria
phone : 21321247913
e-mail: fouzia.zerrouk@gmail.com

Folia Histochem Cytobiol. 2022
10.5603/FHC.a2022.0013
ISSN 0239-8508, e-ISSN 1897-5631

www.journals.viamedica.pl/folia_histochemica_cytobiologica

Keywords: Cardiovascular diseases; Hyperhomocysteinemia; Liver; Methionine; *Psammomys obesus*; SMCs

Introduction

Cardiovascular diseases are complex pathologies with multiple risk factors including genetic predispositions and environmental factors such as diet. These diseases are thus becoming among the leading causes of death and stressors on the healthcare management in these countries [1].

Homocysteine (Hcy) is a highly reactive sulfhydryl-containing amino acid and an intermediate in methionine metabolism. It is produced *via* the demethylation of dietary methionine, which is abundant in animal protein [2]. For instance, an excessive methionine intake in mice and rats animal models leads to a high plasma concentration of Hcy known as hyperhomocysteinemia (Hhcy) [3–5].

In humans, plasma Hcy concentrations ranging from 12 and 100 μmol/L are considered to be indicative of clinically relevant Hhcy [2]. In 1964, Gibson and collaborators reported for the first time the presence of vascular anomalies in patients with homocystinuria (elevated concentration of Hcy in both plasma and urine) [6]. A few years later, in 1969 McCully introduced his Hcy hypothesis which connected Hhcy to an increased risk of atherosclerosis [7]. To date, Hhcy has become an established risk factor for coronary artery diseases, peripheral vascular diseases, myocardial infarction [8], and liver disease [9].

Indeed, decades of investigation in human patients have established a close correlation between Hhcy and cardiovascular diseases and subsequent complications such as heart attacks and strokes have been described previously [10]. Moreover, a diet rich in methionine has been shown to induce cardiovascular system damage through oxidative stress, inflammation, and extracellular matrix remodeling [3, 5].

Psammomys obesus usually lives on a low energy diet (plants mainly rich in water and minerals) in a natural desert habitat, however, when kept in laboratory conditions fed with a rich diet, the animals show metabolic disorders related to high carbohydrates intake [11, 12]. It is an atherosensitive animal which would thus constitute an ideal model for the study of cardiovascular diseases [11, 12]. We previously showed Hhcy to induce a myocardial remodeling including extracellular matrix in *Psammomys obesus* [13], but we did not address the effects of Hhcy on the other components of the cardiovascular system.

Our current work aims to establish a new model for cardiovascular and liver diseases in *Psammomys obesus*. Indeed, *Psammomys obesus* administrated with methionine (Met) induced an Hhcy associated with vascular and liver alterations reproducing cardiovascular and liver pathologies phenotype.

Material and methods

Biological material and experimental protocol. Our study was conducted on an experimental model of gerbillid class (*Psammomys obesus*), gopher, a deserticolous rodent from the region of Beni-Abbes, southwest of Algeria, in the city of Bechar (30°7 northern latitude and 2°10 western longitude). In its natural environment, this gerbil eats halophilic Chenopodiaceae poor in calories (0.4 kcal/g for *Salsola foetida*). The Chenopodiaceae are very rich in water and mineral salts, especially sodium carbonate. *Psammomys* is an animal primarily diurnal, living alone or in small groups in burrows offering shelter from external temperature with high moisture (50–80%) [14].

After familiarization time (25°C with 12-hour light/dark cycles), female animals were divided into two pools, one for control and another experimental: a control pool (n = 5 animals) with a mean bodyweight of 93 g receiving 50 g of halophilic plants daily, and an experimented pool (n = 5 animals) with a mean bodyweight of 96 g receiving daily 50 g of halophilic plants with methionine (Sigma-Aldrich, 64340, St. Louis, MO, USA), previously dissolved in physiological water, at a dose of 70 mg/kg of body weight/day for the treated lot. During the 6 months experiment, the animals were weekly weighted. All experiments were carried out in accordance with the Algerian legislation (Law number 12-235/2012) relating to animal protection, the recommendations of the Algerian Association of Experimental Animal Sciences (AASEA 45/DGLPAG/DVA/SDA/14), and the EU Directive 2010/63/EU for animal experiments.

Blood samples were collected at the beginning (T0) and at the end (T6) of the experiment from the retro-orbital sinus of the eyes using a previously heparinized Pasteur pipette [15]. Blood collected on heparinized tubes was centrifuged at 3000 g for 10 min. The collected plasma was stored at −80°C for the determination of some biochemical plasma parameters.

Determination of total plasma homocysteine. The quantitative determination of total plasma homocysteine was performed by the Architect Homocysteine assay kit (Axis-Shield Diagnostics Ltd, Dundee, UK) using CMIA (chemiluminescent microparticle immunoassay) technology. The oxidized form of homocysteine present in the sample was reduced to free homocysteine by the action of dithiothreitol [16]. Total free homocysteine was transformed into S-adenosyl-L-homocysteine (SAH) by recombinant SAH-hydrolase in the presence of adenosine in excess. SAH and S-adenosyl-L-cysteine labeled with acridinium competed to fill the binding sites on the anti-SAH monoclonal antibody. After

Folia Histochem Cytobiol. 2022
10.5603/FHC.a2022.0013
ISSN 0239-8508, e-ISSN 1897-5631

washing, magnetic separation, and triggering reactions, the light emitted by the acridinium was measured in relative units of light by the optical system of the Architect analyzer. An indirect relationship exists between the homocysteine present in the sample and the amount of light emitted.

Determination of biochemical plasma parameters. Different plasma parameters were quantified by the enzymatic colorimetric method (glucose, triglycerides, cholesterol, total proteins, and uric acid) by using Spinreact kits. Plasma was collected for the measurement of lipoprotein on agarose gel by the method of Kawakami *et al*. (1989).

Histological and histochemical analyses. At the end of the experiment, animals were sacrificed after anesthesia by intraperitoneal injection of urethane 25%. The organs (heart, aorta, and liver) removed were quickly fixed in two different fixing solutions (Bouin's solution and 10% buffered formalin), for 3 days and then dehydrated in ascending series of ethanol. The organs were then cleared in 2 butanol baths and embedded in paraffin. The 5 μm-thick sections were spread on Superfrost-plus glass slides. The slides were subjected to topographic staining (Masson Trichrome method) and selective histochemical staining of collagens and elastin fibrillar (light green), proteoglycans (Alcian blue), glycoproteins (Periodic Acid Schiff), and lipid deposits (Sudan Black) according to described methods [18].

Culture of aortic smooth muscle cells. The SMCs were cultured by the explant technique [19]. The control aorta was removed and immediately plunged in a Petri dish containing Dulbecco's modified Eagle's medium (DMEM) with 10% fetal calf serum (FCS) supplemented with 1% antibiotics (streptomycin 50 mg/mL, penicillin 50 IU/mL, Sigma), 1.2% glutamine (Sigma) and 5% HEPES to maintain Ph of 7.4. The aortic lumen was then emptied of blood. The aorta was incubated for 20 min at 37°C in 0.1% collagenase I (Sigma) in a serum-free medium to remove the endothelium and facilitate the separation of adventitia and media and cut into 1 mm explants. 8–10 explants were placed in culture 25 cm^3 flasks and incubated in the presence of DMEM containing 20% FCS, 1.2% glutamine, and 1% antibiotics and placed in the incubator at 37°C under a humidified atmosphere with 95% air and 5% CO_2. The cultivation of explants is the primary culture.

On the second culture passage and at the 7th passage and at a confluence, the cells were resuspended after trypsinization. They have seeded in 6-well plates at a rate of 0.8×10^6 cells/ /mL/well in DMEM supplemented with 10% FCS, 1.2% glutamine, and 1% antibiotics and incubated in the presence of 50 mM methionine for 72 h [20]. At confluence, the medium was removed; the control SMCs and SMCs cultured with methionine were reincubated in 1.5 mL DMEM without FCS for 24 h. The mediums were used for the determination of total protein [21].

Quantification of aortic smooth muscle cells proliferation rate. The SMCs were seeded in 6-well plates at a rate of 0.8×10^6 cells/mL/well in DMEM supplemented with 10% FCS, 1.2% glutamine, 1% antibiotics. Six SMCs plated well were treated with 50 mM of methionine and incubated for 72 h [20]. Another six SMCs plated wells were incubated without methionine and used as control. The cell proliferation rate was then performed on 100 μL cell suspension in the presence of trypan blue by counting in Malassez chamber.

Morphometric analyses of heart and aorta. The morphometric study of the organ's structure was performed, using a Zeiss-type micrometer. For each of the parameters studied, we carried out 50 measurements on different fields of several histological sections, corresponding to the different control and treated animals. The microphotographs were made with Zeiss Primo Star type photomicroscope.

In the heart, we determined the thickness of the endocardium, myocardium, and pericardium. In the aorta, we measured thickness (arterial wall, intima, media, adventitia, and interlamellar spaces), number of elastic laminae, number of SMCs nuclei, and the dimensions of SMCs nuclei (length of their major and minor axes).

Morphometry of cultured aortic smooth muscle cells. To analyze the effect of methionine on SMCs (7th passage), the cells were plated in 6-well plates at 0.8 x 10^6 cells/mL/well in the presence of methionine (50 mM) for 72 h. After this period the *milieu* was removed, and the cells were washed once in phosphate-buffered saline (PBS) and fixed in Bouin's fixative for 30 min. After rinsing with PBS and ethanol (96%), the cells were stained for 10 min with a solution of Giemsa (1% in methanol) and May Grunwald (0.7g/L) (V/V, 1:1) stains, diluted to 1/3 in distilled water. The excess of stain was removed by washing with PBS.

In order to assess the phenotypic state of SMCs (synthetic and contractile) subjected to methionine, we carried out 25 measurements concerning certain cellular and nuclear parameters, namely, cellular major axis, major and small nuclear axes, number of nucleoli in each nucleus and nuclear major axis/cellular major axis ratio of SMCs. Each parameter was measured in different fields of view and in several wells.

Statistical analysis. Quantitative results were analyzed by GraphPad Prism 8.0 software (GraphPad Inc., San Diego, CA, USA). The values were expressed as a mean and mean's standard error (SEM). The Mann-Whitney test was used to evaluate the difference between the parameters of control and treated animals. Student's *t*-paired test was used for SMCs culture study. When the values of P were

lower than 0.05, the difference was considered statistically significant.

Results

Chronic methionine administration induced hyperhomocysteinemia in Psammomys obesus

We first sought to determine whether daily methionine treatment over 6 months induced Hhcy in *Psammomys obesus*. The Hcy concentration was measured, using chemiluminescent microparticle immunoassay, at day 1 before any injection of methionine to determine the baseline value of homocysteinemia of *Psammomys obesus* and 6 months later at the end of the experiment to assess the final homocysteinemia state.

A daily intraperitoneal injection of 70 mg/kg of methionine induced a large and significant increase of 529.93% ($P < 0.001$) in plasma homocysteinemia after 6 months. From 3.24 ± 0.84 μmol/L at day 1, homocysteinemia raised to 20.41 ± 5.39 μmol/L which is considered being a moderate range of Hhcy (Fig. 1).

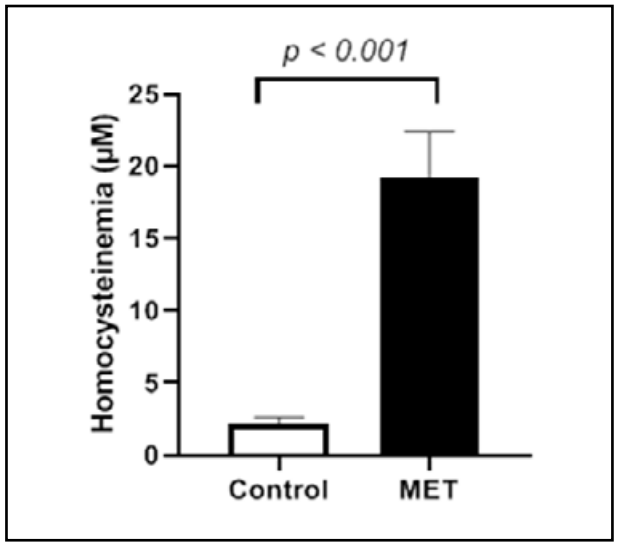

Figure 1. Plasma homocysteine concentrations in the control and methionine-administered (Met) female sand rats, after 6 months of the experiment's duration. Data are presented as mean ± SD ***statistically significant differences between the control (n = 5) and methionine (n = 5) group, $P < 0.001$

Methionine-mediated hyperhomocysteinemia induced an increase of atherogenic lipoproteins in plasma of Psamomomys obesus

Atherosclerosis is among the most prevalent cardiovascular pathologies, which is related to lipid deposits in the wall of arteries. We next investigated the effect on atherosclerosis plasma markers and risk factors of methionine-mediated Hhcy at 6 months. Methionine treatment induced a significant increase in plasma glucose and uric acid concentrations (increases of 32.78% and 105.6%, respectively) (Table 1). The treatment with methionine also induced a large increase in triglyceridemia (307.36%; $P < 0.001$), whereas the increase in cholesterolemia by 45.37% was not significant (Table 1). The methionine treatment induced a decrease in the HDL-lipoproteins level (70.4%; $P < 0.01$) and a tendency to an increase in the atherogenic lipoproteins LDL-VLDL plasma concentration (35.1%; $P > 0.05$) (Table 1). Moreover, we detected the presence of lipoprotein (a), a highly atherogenic LDL. Methionine-induced Hhcy was also accompanied by a decrease in bodyweight (Table 1).

Histological alterations of organ structure induced by methionine-mediated hyperhomocysteinemia

The heart

The methionine-mediated Hhcy resulted in the significant thickening of *Psammomys obesus* heart's endocardium, myocardium, and pericardium (Table 2 and Figs. 2C, E, F, K).

Table 1. Evolution of body weight and biochemical plasma parameters in control and methionine-treated sand rats

Parameters	Time 0 values	After 6 months of methionine (Met) administration at a dose of 70 mg/kg/day	
		Control group (n = 5)	Met group (n = 5)
Body weight (g)	94.75 ± 18.58	105.5 ± 3.97	88.63 ± 5.94*
Glycemia (mg/dL)	77.14 ± 11.77	48.42 ± 9.37	102.43 ± 29.62*
Triglyceridemia (mg/dL)	48.05 ± 19.41	54.9 ± 32.22	195.74 ± 90.82***
Cholesterolemia (mg/dL)	49.67 ± 7.47	52.2 ± 17.71	72.21 ± 47.02
HDL (mg/dL)		59.2 ± 7.2	17.54 ± 19.45**
LDL-VLDL (mg/dL)		50.27 ± 7.2	67.92 ± 31.33
Lipoprotein (a) (mg/dL)		Not detectable	14.58 ± 15.33
Proteinemia (mg/dL)	64.37 ± 19.08	48.8 ± 2.59	73.4 ± 9.82
Uric acid (mg/dL)	6.6 ± 2.19	5.84 ± 2.06	13.57 ± 4.8***

Data are presented as mean ± SD. *, **, *** statistically significant differences between the control and methionine group, $P < 0.05$, $P < 0.01$ and $P < 0.001$, respectively. Plasma levels of HDL, LDL-VLDL and Lp (a) were not measured at time 0.

Folia Histochem Cytobiol. 2022
10.5603/FHC.a2022.0013
ISSN 0239-8508, e-ISSN 1897-5631

Table 2. Morphometric parameters of the heart wall layers in control and methionine-treated (Met) sand rats

Morphometric parameters	Control group	Met group
Endocardium thickness (μm)	1.16 ± 0.40	4.05 ± 1.59****
Myocardium thickness (μm)	1468.89 ± 360.95	2298.22 ± 306.07****
Pericardium thickness (μm)	3.54 ± 1.97	38.73 ± 26.95****

Data are presented as mean ± SD. ****statistically significant differences between the control and Met- group after 6 months of the experiment's duration; $P < 0.0001$ (n = 5; 6 sections per animal).

However, while the increase in endocardium and myocardium thickness was associated with an accumulation of connective tissue components (Figs. 2C, H, I), the increase in epicardium thickness seems to be secondary to an edema formation (Fig. 2K). Moreover, the endocardium exhibited endothelial cells hypertrophy and microthrombi on the luminal surface (Fig. 2B). The myocardium layer appeared disorganized with enlarged intercellular spaces with a cellular infiltration between the cardiomyocytes' fibers (Fig. 2F) and some cardiomyocytes exhibiting a pyknotic nucleus (Fig. 2E).

The aorta

Similarly, to the observations in the cardiac tissue, the methionine-mediated Hhcy caused significant alterations in the three layers of the aortic wall (intima, media, and adventitia) at both cellular and matrix levels. The thickness of the aortic wall increased significantly in the methionine-treated animals compared to the control group with an intima increase of 34.74% ($P < 0.001$) (Table 3). In addition, methionine treatment-induced microthrombi formation on the luminal surface (Fig. 3B), endothelial cell hypertrophy (Fig. 3B), stronger staining of the internal elastic lamina (Figs. 3C1, C2), and the remodeling of the extracellular matrix of the aortic wall (Figs. 3D, E, F, H).

The media layer of the aorta of methionine-treated animals presented thinner elastic laminas with a much less "wavy aspect" and focal ruptures (Figs. 3D, E). Moreover, collagen accumulated both at the periphery of the elastic lamina and in the interlamellar spaces (Figs. 3E, F) resulting in a significant increase in these spaces (23.84%, $P < 0.01$). Interestingly, the SMCs of methionine-treated animals exhibited two different phenotypes: proliferative SMCs (Fig. 3G) and reoriented SMCs (Fig. 3F) with a significant decrease in the major axis compared to the control group (Table 3). Methionine-induced Hhcy in *Psammomys obesus* also led to aneurysms' formation that was marked by large fibrosis in the media and adventitia which increased their thickness (Fig. 3H).

The liver

Similarly to cardiovascular structural alterations observed in methionine-treated animals, the liver's structure showed deep alterations characterized by the presence of hepatocytes with pycnotic nuclei (Fig. 4F), an accumulation of connective tissue components including collagens (Fig. 4C), glycoproteins (Fig. 4D), and proteoglycans (Fig. 4E) between the hepatocytes (Fig. 4F) and around the vessels causing a thickening of their walls and forming perivascular fibrosis. In addition to these alterations, methionine-induced Hhcy resulted in a true hepatic steatosis state (Fig. 4F, G) with the majority of the hepatocytes stuffed with lipids droplets (Fig. 4H) giving the liver a spongy aspect, light in color compared to the brown shade of a normal liver.

Effects of methionine on cultured aortic smooth muscle cells

After 72 h of incubation with methionine (50 mM), the SMCs primary cultures exhibited the two phenotypes: fusiform contractile quiescent SMCs (Fig. 5C) and polygonal synthetic proliferative state (Fig. 5D). However, the quantification of the proliferation rate of SMCs showed no significant increase in the proliferation of the cells after methionine treatment compared to control cells (Fig. 5E; Table 4) while the assessment of the total protein in the extracellular compartment was significantly increased after methionine treatment suggesting an increase in protein secretion by SMCs (0.13 ± 0.02 *vs.* 0.07 ± 0.01 μg/mL, $P < 0.001$) (Fig. 5F).

In addition, the SMCs of the two subpopulations became significantly larger after 72 h of methionine treatment, by 44.72% ($P < 0.0001$) in contractile SMCs (Fig. 5C), and 18.12% ($P < 0.001$) in synthetic SMCs (Fig. 5D; Table 4). The SMCs nuclei also significantly increased in size, by 22.98% ($P < 0.0001$) in contractile SMCs and 16.11% ($P < 0.0001$) in synthetic SMCs (Table 4). In addition to the bigger size, the nuclei of the synthetic SMCs showed an increased number of nucleoli compared to corresponding controls (3.4 ± 0.97 *vs.* 2.92 ± 0.67, $P < 0.01$) (Table 4).

Discussion

Red meat, a component of the routine diet, contains high methionine level which is absorbed very efficiently and enters the plasma until removed and metabo-

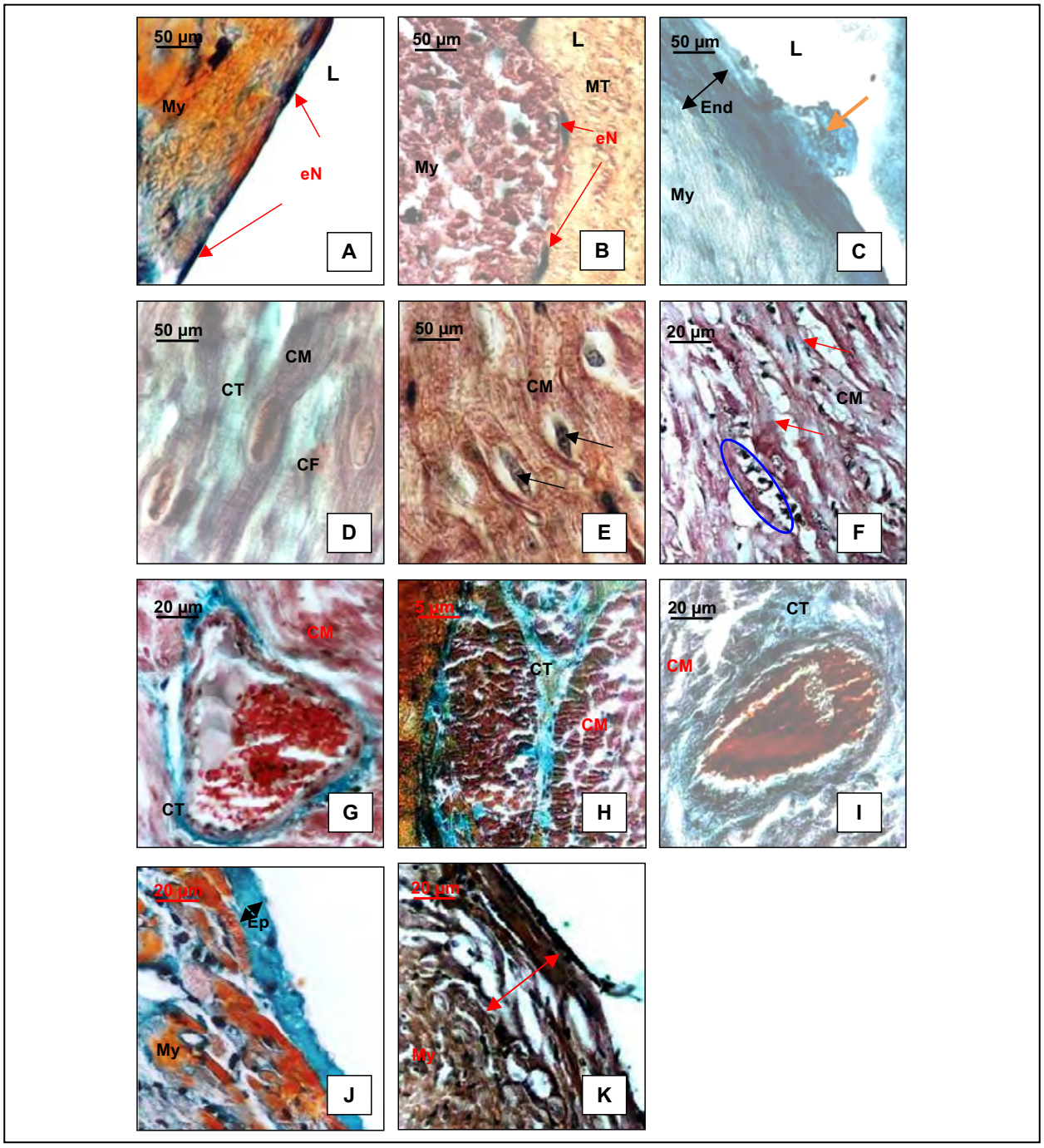

Figure 2. Heart morphology of the control (A, D, G, J) and methionine-administered (Met) female sand rats (B, E, F, H, I, K), after 6 months of the experiment's duration; **A.** Endocardium of control sand rat; **B.** Endocardium of rat from Met group: hypertrophy of endothelial cells (red arrow) and microthrombus on the luminal surface; **C.** Endocardium of rat from methionine group: deposition of extracellular matrix material (proteoglycans) (black arrow), appearance of a protuberance on the luminal side (orange arrow); **D, G.** Myocardium of control rat: cardiomyocytes surrounded by weakly vascularized connective tissue composed of a few collagen fibers and many cardiac fibroblasts; **E.** Myocardium of methionine group: a jagged shape of cardiomyocytes' nuclei with dense chromatin (black arrows); **F.** Myocardium of methionine-treated group; an enlargement of the intercellular spaces (red arrow), cellular infiltration between the cardiomyocytic trabeculae (blue circle); **H, I.** Myocardium of methionine group; interstitial and perivascular fibrosis; **J.** Epicardium of control sand rat: it covers the myocardium on the outside (black arrow); **K.** Epicardium of methionine group is characterized by a thickening (red arrow) marked by the presence of empty spaces. Abbreviations: L — lumen; eN — endothelial cell nucleus; My — myocardium; MT — microthrombus; CM — cardiomyocytes; CT — connective tissue; CF — cardiac fibroblasts. Sections were stained with Masson trichrome except for section C stained with alcian blue. Scale bars: 50 μm (A, B, C, D and E); 20 μm (F, G, I, J and K); 5 μm (H).

Folia Histochem Cytobiol. 2022
10.5603/FHC.a2022.0013
ISSN 0239-8508, e-ISSN 1897-5631

Table 3. Morphometric parameters of the aortic wall layers in control and methionine-treated (Met) sand rats

Morphometric parameters	Control group	Met group
Wall thickness (μm)	119.8 ± 15.95	144.94 ± 57.86**
Adventitia thickness (μm)	30.25 ± 16.14	43.48 ± 59.38
Media thickness (μm)	87.75 ± 8.43	100.30 ± 24.53***
Intimal thickness (μm)	2.13 ± 0.58	2.87 ± 1.25***
Interlamellar space thickness (μm)	7.55 ± 2.97	9.35 ± 3.77 **
Major axis of SMCs (μm)	8.03 ± 2.80	6.58 ± 2.14***
Small axis of SMCs (μm)	3.28 ± 1.15	3.33 ± 1.12
Number of nuclei of SMCs (per 5625 μm^2)	11.32 ± 3.29	15.06 ± 3.34****
Number of elastic laminas	7.48 ± 0.91	7.34 ± 1.04

Data are presented as mean ± SD. **,***,****statistically significant differences between the control and Met- group after 6 months of the experiment's duration; $P < 0.01$, $P < 0.001$ and $P < 0.0001$, respectively (n = 5; 10 sections *per* animal).

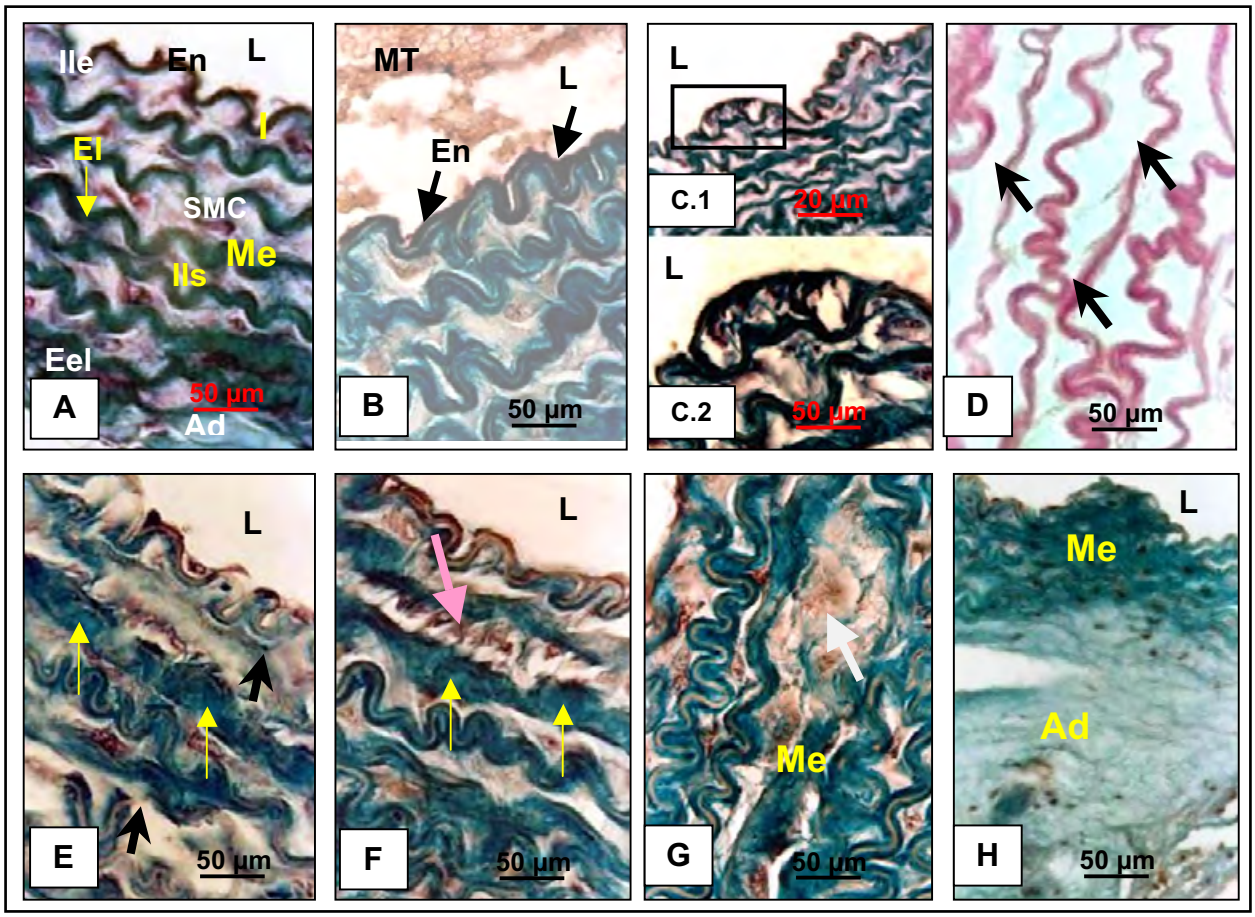

Figure 3. Aorta histology of the control (**A**) and methionine-administered (Met) female sand rats (**B, C, D, E, F, G, H, I**), after 6 months of the experiment's duration; **A.** Aorta of control sand rat; **B.** Aorta of Met group; microthrombus and hyperplasia of endothelial cells (black arrow); **C.** Increased spaces in the intima probably reflecting local edema (**C1**) and duplication of internal elastic lamina (**C2**); **D.** Undulation shape loss, thinning of the elastic laminas; **E.** Breakage of elastic laminas (black arrow); **E, F.** Accumulation of collagen (yellow arrow); **F.** SMCs migration (pink arrow); **G.** SMCs proliferation (white arrow); **H.** Fibrosis in the media and the adventitia, installation of the aneurysm. Abbreviations: L — lumen; I — intima; En — endothelium; Ile — internal elastic lamina; El — elastic lamina; Ils — inter-lamellar space; SMCs — smooth muscle cells; Me — media; Eel — external elastic lamina; Ad — adventitia; MT — microthrombus. Sections were stained with Masson's trichrome except for section D with PAS staining. Scale bars: 50 μm.

Folia Histochem Cytobiol. 2022
10.5603/FHC.a2022.0013
ISSN 0239-8508, e-ISSN 1897-5631

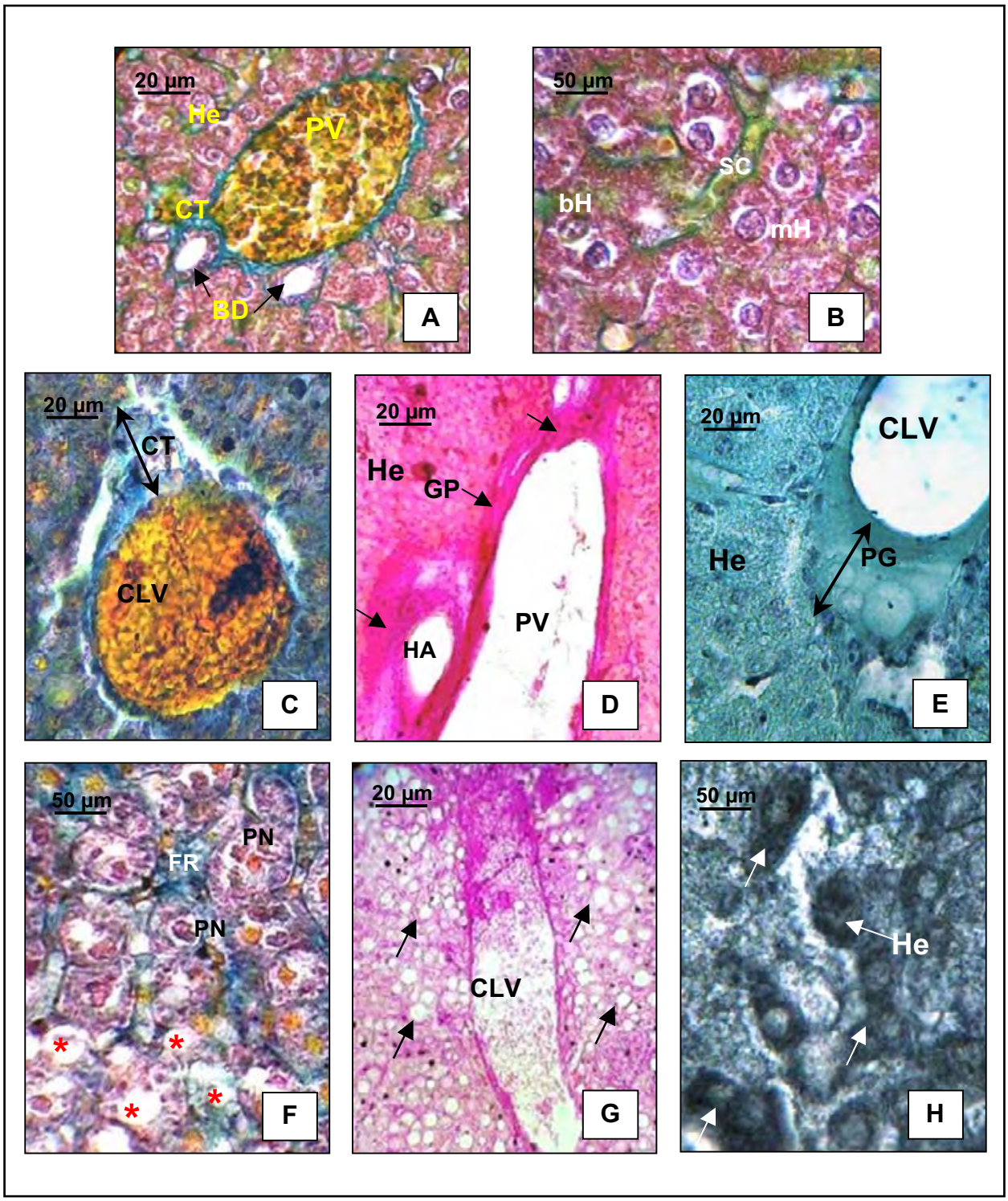

Figure 4. Liver histology of the control (**A**, **B**) and methionine- administered female sand rats (**C–I**), after 6 months of the experiment's duration; **A**. A portal space in the hepatic tissue of control sand rat; **B.** The hepatic tissue is made up of lobules with mononuclear and binuclear hepatocytes; **C.** Accumulation of perivascular connective tissue in the liver of methionine group; **D.** Accumulation of glycoproteins; **E.** Accumulation of proteoglycans; **F.** Installation of interstitial fibrosis and vacuolation of the cytoplasm (*); presence of hepatocytes with pyknotic nuclei; **G.** Installation of hepatic steatosis (black arrow); **H.** Lipid deposition (black arrow). Abbreviations: He — hepatocyte; PV — portal vein; BD — bile duct; CT — connective tissue; SC — sinusoid capillaries; mH — mononuclei hepatocyte; bH — binucleated hepatocyte; CLV — sublobular vein; HA — hepatic artery; GP — glycoproteins; PG — proteoglycans; PN — pyknotic nuclei; FR — fibrosis. Stainings: A, B, C and F: Masson's trichrome method; D and G: PAS; E: alcian blue; H: Sudan Black. Scale bars: 20 μm (A, C, D, E and G); 50 μm (B, F and H).

Folia Histochem Cytobiol. 2022
10.5603/FHC.a2022.0013
ISSN 0239-8508, e-ISSN 1897-5631

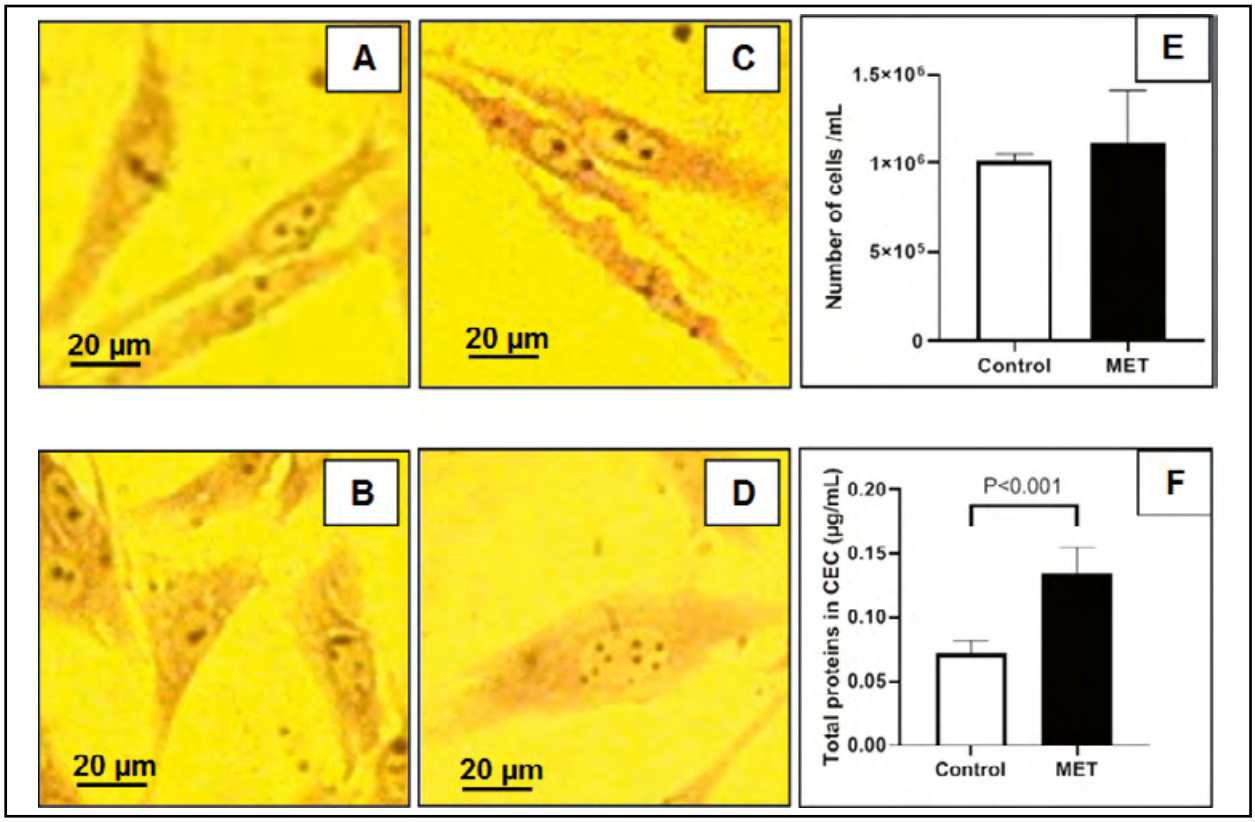

Figure 5. *Psammomys obesus* aortic smooth muscle cells (SMCs) of control group (**A, B**) and SMCs treated with 50 mM methionine (**C, D**) for 72 hours; **A.** Contractile SMCs of control group; **B.** Synthetic SMCs of control group; **C**. Contractile SMCs of Met-group; **D**. Synthetic SMCs of Met-group; **E**. Proliferation SMCs Met-group *vs* control group; **F**. Total protein ($\mu g/10^6$ cells) in the extracellular compartment of SMCs Met-group *vs* control group. Data are presented as mean ± SD; *** statistically significant differences between the control and Methionine group; $P < 0.001$.

Table 4. Morphometric study of the cultured aortic smooth muscle cells (SMCs) of contractile and synthetic phenotypes, in control cells and methionine-treated cells

	Contractile SMCs		**Synthetic SMCs**	
Morphometric parameters	Control group	Methionine group	Control group	Methionine group
Cellular major axis (μm)	72.18 ± 15.82	104.46 ± 29.08****	46.02 ± 9.10	54.36 ± 12.74***
Nuclear major axis (μm)	15.66 ± 2.66	19.26 ± 3.98****	14.52 ± 2.02	16.86 ± 2.9****
Nuclear small axis (μm)	7.62 ± 1.51	9.87 ± 2.57****	12.72 ± 1.55	13.59 ± 2.09*
Nuclear axis/cellular axis	0.22 ± 0.05	0.19 ± 0.05***	0.33 ± 0.07	0.32 ± 0.08
Number of nucleoli	2.56 ± 0.97	2.64 ± 0.90	2.92 ± 0.67	3.4 ± 0.97**

Data are presented as mean ± SD. *, **, ***, ****statistically significant differences at the same time between the control and methionine-treated cells at 50 mM for 72 h; $P < 0.05$, $P < 0.01$, $P < 0.001$ and $P < 0.0001$, respectively (n = 2; 6 sections per animal).

lized by the different tissues [3]. Since the cardiovascular disease increases in the population with high meat intake, the question is raised whether methionine directly or through its metabolites is implicated in the pathophysiology of cardiovascular diseases. For instance, given that methionine is a donor of methyl groups, it has been shown that excess of methionine in diet content alters the DNA methylation levels thus altering the gene expression [22]. More importantly, the accumulation of Hcy, a methionine-derived metabolite, causing Hhcy has been demonstrated to be a cardiovascular disease risk [3, 23].

Numerous experimental data have indicated that Hhcy can result from either Hcy [24, 25] or methionine supplementation [26, 27]. In our model, we aimed to induce chronic moderate hyperhomocysteinemia with a daily methionine intraperitoneal injection at a dose of 70 mg/kg in *Psammomys obesus* for 6 months.

The treatment induced a moderate-level Hhcy (20.41 ± 5.39 μmol/L) considering the values reported in human plasma that ranges from 12 to 30 μmol/L [2]. However, to induce a moderate Hhcy in humans, only a single oral high dose of methionine was necessary (0.1 g/kg) [28]. Our result is in agreement with those reported by many previous studies that showed a methionine-enriched diet to induce a moderate Hhcy in different animal models (pig, gerbil, and rat) [27, 29, 30]. In the rat, a species known to be athero-resistant administration of a high dose of methionine (200 mg/kg) for a long period (6 months) is necessary to induce Hhcy [31, 32]. In our laboratory, a study published in 2019, reported for the first time a moderate Hhcy in *Psammomys obesus*; however, the Hhcy was induced by a high dose of methionine (300 mg/kg) administered for 4 weeks [13]. Our current model, in contrast to the previous models using a high dose of methionine for a short period of time, shows that administration of a low dose of methionine for a long time is sufficient to induce Hhcy in *Psammomys obesus* and thus better reproduces the slow progressive disease occurrence in human pathology.

We first investigated the body weight of the animal every month during the 6 months of methionine administration and reported a significant decrease from the 2nd month to the end of the experiment. Similar results were reported by Ghoul and Zhou in rats and mice respectively [32, 33]. However, the bodyweight seems to be not always affected in rats and gerbils by methionine-induced Hhcy [26, 30, 31] and it is plausible that the variations in the dose of methionine and duration of its administration may play a role.

In our model, the methionine-induced Hhcy was associated with significant hyperglycemia increased uric acid concentration, and dyslipidemia all of which parameters are included in human metabolic syndrome phenotype and implicated in cardiovascular disease pathophysiology. Some of these alterations including hyperglycemia and uric acid increase were not observed in previous models [13, 29, 31]. Moreover, we found that a significant increase in triglyceridemia in the methionine-mediated Hhcy animals was associated with a misbalance between a decreased plasma cardioprotective lipoprotein HDL level and increased concentration of the plasma atherogenic lipoprotein LDL-VLDL including the lipoprotein a. Our results are in agreement with those observed in the well-known atherosclerosis mouse model ApoE-/- in which the gene coding the CBS (cystathionine beta-synthase, the enzyme degrading Hcy) was also inactivated to induce Hhcy [34]. The presence in the blood plasma of lipoprotein a, considered a cardiovascular disease factor risk [35], and in methionine-induced Hhcy animals further confirms the relevance of our model to assess cardiovascular diseases pathophysiology mechanisms such as oxidative stress [36] and inflammation [37] and the efficiency of new therapies directed against homocysteinemia. This therapeutic target is underlined by findings that revealed that plasma Hcy level positively correlated with remodeling of extracellular matrix (ECM) of several tissues, including the heart, aorta, and liver [38, 39].

The structural alterations in the heart, aorta, and liver in *Psammomys obesus* animals administrated with 70 mg/kg of methionine for 6 months further characterized the atherosclerosis phenotype induced by Met-mediated Hhcy. Indeed, methionine-induced Hhcy exerted angiotoxic effects on the heart and aorta characterized by the presence of microthrombi, atheromatous plaques, interstitial and perivascular fibrosis in addition to deep alterations in the myocardium and liver steatosis. Similar alterations were previously observed after methionine treatment in different animal models including *Psammomys obesus*; however, the doses of methionine were 2.5 to 4 times higher than in the current study [4, 13, 31, 40, 41]. Moreover, in the previous study in *Psammomys obesus*, the high methionine administration was administrated for a short period (30 days) reproducing an acute Hhcy and its subsequent effects [13].

Interestingly, our current study showed that the interstitial and the perivascular fibrosis in the myocardium is due to the accumulation of collagen type I and type III confirming our previous results [13] that demonstrated this accumulation was associated with an imbalance between increased expression of MMP-9 metalloproteinase and tissue inhibitor of metalloproteinases 2 (TIMP-2) and decreased expression of MMP-2 and TIMP-1. Moreover, the cellular infiltration between the cardiomyocytic trabeculae suggested the presence of inflammation. Indeed, we previously showed an increase in plasma CRP level in *Psammomys obesus* treated with a high dose of methionine for one month [13]. This inflammatory marker was also reported to be increased in a dose- and time-dependent manner in rats treated with methionine [26]. Furthermore, the thickening of the epicardium in the methionine-mediated Hhcy *Psammomys obesus* group suggested either edema or an accumulation of adipose tissue [42].

The aorta is the main vascular structure after the heart. Here we show that Met-mediated Hhcy induced deep alterations of the aorta including intima layer thickening and hyperplasia of the endothelial cells, which suggest subsequent vascular dysfunctions. Indeed, the thickening of the sub-endothelial space presents a fibrous material rich in collagen indicating

Folia Histochem Cytobiol. 2022
10.5603/FHC.a2022.0013
ISSN 0239-8508, e-ISSN 1897-5631

the formation of young atheromatous plaques while the observed endothelial lesions and ruptures of *elastica interna* would increase the intimal permeability to macromolecules allowing their accumulation in the intima layer [33]. Previous studies showed these alterations to be associated with an increase in adhesion molecules expressed in the aorta wall such as ICAM-1, E-selectin, and P-selectin [42–45]. The increase in these molecules has been shown to subsequently induce an increased adhesion of monocytes to aortic endothelium [43–46].

Consistently with Augier and collaborators' results [47] we observed, in the methionine-mediated Hhcy, a thinning of the aortic media layer together with the loss of undulation, disorganization, and disruption of elastic laminas reflecting vascular remodeling and damage of elastic fibers' network. Some authors suggested this damage associated with short elastin fragments could result from the increase in elastase-like activity dependent on metalloproteinases [41, 48].

Importantly, methionine-mediated Hhcy induced the proliferation and migration of SMCs in some interlamellar space areas with complete disorganization of the matrix and collagen accumulation. Indeed, from a quiescent contractile phenotype in control animals, the SMCs isolated from methionine-treated animals showed synthetic or proliferative phenotypes. The transition of SMCs between the two phenotypes was shown to be associated with human atherosclerosis pathology [49]. Moreover, previous *in vivo* and *in vitro* studies have shown methionine or Hcy treatment to induce SMCs proliferation and migration, partially due to p38 activation or increased expression of *cyclin D1* and *cyclin A* mRNA transcripts [25, 50–52].

In the aortal adventitia, we noticed a matrix very rich in collagen probably synthesized by fibroblasts. Yao and Sun (2014) demonstrated that incubation of rat aortic adventitial fibroblasts with Hcy significantly increased collagen type 1 and AT1R (Angiotensin II Type 1 Receptor) expression [53], suggesting that adventitial fibroblasts may play an important role in the accumulation of the extracellular matrix and vascular adventitial remodeling. Our results also showed an association between increased levels of Hcy and the occurrence of an aneurysm. According to Liu *et al.* (2012), Hhcy induces abdominal aortic aneurysm formation in mice *via* activation of the adventitial fibroblast NADPH oxidase 4 [54].

Hhcy is well known as an independent risk factor for cardiovascular disease [8, 55], and has been proposed to be a potential risk factor for nonalcoholic fatty liver disease [5, 56]. Hepatic steatosis is due to increased lipids' uptake, biosynthesis, or impaired lipids export in addition to fatty acids oxidation in mitochondria. Interestingly, our study showed methionine-mediated Hhcy to induce deep hepatic steatosis with the majority of hepatocytes packed with lipid droplets and adipose tissue accumulation in interstitial and perivascular spaces. In agreement with our results, Ai *et al*. (2017) demonstrated, that 16 weeks of high methionine diet feeding (2% of methionine) in C57BL/6J mice, increased plasma Hcy level and induced hepatic steatosis [57]. The same results were observed in rats administrated high methionine diet (500 mg/kg/day) for three months [4]. In addition to lipids accumulation, the pathogenesis of liver diseases in the case of hyperhomocysteinemia could be due to the excessive generation of reactive oxygen species [58, 59]. Indeed, some studies on rat liver have shown that a methionine-rich diet increases hepatic lipid peroxidation [60, 61], and decreases the antioxidant activity [62].

In summary, we found that prolonged methionine administration in *Psammomys obesus* induced hyperhomocysteinemia associated with an atherosclerosis phenotype including the typical alterations observed in the heart, aorta, and liver. Therefore, we suggest that our experimental model could be used for better understanding atherosclerosis pathomechanisms and also for testing anti-atherosclerotic therapies.

Financial disclosure

This study was supported by the PRFU project D01N01UN160420180008 (DGRSDT-Ministry of Higher Education and Scientific Research. Algeria).

Conflicts of interest

The authors declare no conflict of interest.

References

1. Rabinovich-Nikitin I, Lieberman B, Martino TA, et al. Circadian-Regulated Cell Death in Cardiovascular Diseases. Circulation. 2019; 139(7): 965–980, doi: 10.1161/CIRCULATIONAHA.118.036550, indexed in Pubmed: 30742538.
2. Guilland JC, Favier A, Courcy GP, et al. L'hyperhomocystéinémie : facteur de risque cardiovasculaire ou simple marqueur ? Pathologie Biologie. 2003; 51(2): 101–110, doi: 10.1016/s0369-8114(03)00104-4.
3. Chaturvedi P, Kamat PK, Kalani A, et al. High Methionine Diet Poses Cardiac Threat: A Molecular Insight. J Cell Physiol. 2016; 231(7): 1554–1561, doi: 10.1002/jcp.25247, indexed in Pubmed: 26565991.

4. Yefsah-Idres A, Benazzoug Y, Otman A, et al. Hepatoprotective effects of lycopene on liver enzymes involved in methionine and xenobiotic metabolism in hyperhomocysteinemic rats. Food Funct. 2016; 7(6): 2862–2869, doi: 10.1039/c6fo00095a, indexed in Pubmed: 27232443.
5. Stojanović M, Todorović D, Šćepanović Lj, et al. Subchronic methionine load induces oxidative stress and provokes biochemical and histological changes in the rat liver tissue. Mol Cell Biochem. 2018; 448(1-2): 43–50, doi: 10.1007/s11010-018-3311-2, indexed in Pubmed: 29423685.
6. Gibson JB, Carson NA, Neill DW. Pathological findings in homocystinuria. J Clin Pathol. 1964; 17: 427–437, doi: 10.1136/jcp.17.4.427, indexed in Pubmed: 14195630.
7. Yang F, Tan HM, Wang H. Hyperhomocysteinemia and atherosclerosis - An overview. Int J Pharma Bio Sci. 2011; 2: 348–354.
8. Maron BA, Loscalzo J. The treatment of hyperhomocysteinemia. Annu Rev Med. 2009; 60: 39–54, doi: 10.1146/annurev.med.60.041807.123308, indexed in Pubmed: 18729731.
9. Roblin X, Pofelski J, Zarski JP. Rôle de l'homocystéine au cours de la stéatose hépatique et de l'hépatite chronique C. Gastroentérologie Clinique et Biologique. 2007; 31(4): 415––420, doi: 10.1016/s0399-8320(07)89402-4.
10. Baszczuk A, Kopczyński Z. Hyperhomocysteinemia in patients with cardiovascular disease. Postepy Hig Med Dosw (Online). 2014; 68: 579–589, doi: 10.5604/17322693.1102340, indexed in Pubmed: 24864108.
11. Hamlat N, Negazzi S, Forcheron F, et al. Lipogenesis in arterial wall and vascular smooth muscle cells of Psammomys obesus: its regulation and abnormalities in diabetes. Diabetes Metab. 2010; 36(3): 221–228, doi: 10.1016/j.diabet.2010.01.003, indexed in Pubmed: 20303812.
12. Berdja S, Smail L, Saka B, et al. Glucotoxicity induced oxidative stress and inflammation in vivo and in vitro in psammomys obesus: involvement of aqueous extract of brassica rapa rapifera. Evid Based Complement Alternat Med. 2016; 2016: 3689208, doi: 10.1155/2016/3689208, indexed in Pubmed: 27047569.
13. Chaouad B, Moudilou EN, Ghoul A, et al. Hyperhomocysteinemia and myocardial remodeling in the sand rat, Psammomys obesus. Acta Histochem. 2019; 121(7): 823–832, doi: 10.1016/j.acthis.2019.07.008, indexed in Pubmed: 31377002.
14. Daly M, Daly S. On the feeding ecology of psammomys obesus (rodentia, gerbillidae) in the wadi saoura, algeria. Mammalia. 1973; 37(4), doi: 10.1515/mamm.1973.37.4.545.
15. Aouichat Bouguerra S, Benazzoug Y, Bekkhoucha F, et al. Effect of high glucose concentration on collagen synthesis and cholesterol level in the phenotypic modulation of aortic cultured smooth muscle cells of sand rat (Psammomys obesus). Exp Diabesity Res. 2004; 5(3): 227–235, doi: 10.1080/15438600490489793, indexed in Pubmed: 15512791.
16. Frantzen F, Faaren AL, Alfheim I, et al. Enzyme conversion immunoassay for determining total homocysteine in plasma or serum. Clin Chem. 1998; 44(2): 311–316, indexed in Pubmed: 9474030.
17. Kawakami K, Tsukada A, Okubo M, et al. A rapid electrophoretic method for the detection of serum Lp(a) lipoprotein. Clin Chim Acta. 1989; 185(2): 147–155, doi: 10.1016/0009-8981(89)90037-5, indexed in Pubmed: 2533887.
18. Martoja R, Martoja M. Initiation aux techniques de l'histologie animale. Paris: Masson. ; 1967.
19. Bouguerra SA, Bourdillon MC, Dahmani Y, et al. Non insulin dependent diabetes in sand rat (Psammomys obesus) and production of collagen in cultured aortic smooth muscle cells. influence of insulin. Int J Exp Diabetes Res. 2001; 2(1): 37–46, doi: 10.1155/edr.2001.37, indexed in Pubmed: 12369725.
20. Benavides MA, Oelschlager DK, Zhang HG, et al. Methionine inhibits cellular growth dependent on the p53 status of cells. Am J Surg. 2007; 193(2): 274–283, doi: 10.1016/j.amjsurg.2006.07.016, indexed in Pubmed: 17236862.
21. Hildebrandt S, Steinhart H, Paschke A, et al. A rapid and sensitive method for the quantitation of microgram quantities of protein utilizing the principle of protein-dye binding. Anal Biochem. 1976; 72(3): 248–254, doi: 10.1006/abio.1976.9999, indexed in Pubmed: 942051.
22. Park CM, Cho CW, Rosenfeld ME, et al. Methionine supplementation accelerates oxidative stress and nuclear factor kappaB activation in livers of C57BL/6 mice. J Med Food. 2008; 11(4): 667–674, doi: 10.1089/jmf.2007.0146, indexed in Pubmed: 19053858.
23. Steed MM, Tyagi SC. Mechanisms of Cardiovascular Remodeling in Hyperhomocysteinemia. Antioxid Redox Signal. 2011; 15(7): 1927–1943, doi: 10.1089/ars.2010.3721, indexed in Pubmed: 21126196.
24. Miller A, Mujumdar V, Shek E, et al. Hyperhomocyst(e)inemia induces multiorgan damage. Heart Vessels. 2000; 15(3): 135–143, doi: 10.1007/s003800070030, indexed in Pubmed: 11289502.
25. Akasaka K, Akasaka N, Di Luozzo G, et al. Homocysteine promotes p38-dependent chemotaxis in bovine aortic smooth muscle cells. J Vasc Surg. 2005; 41(3): 517–522, doi: 10.1016/j.jvs.2004.12.043, indexed in Pubmed: 15838488.
26. Sharma M, Rai SK, Tiwari M, et al. Effect of hyperhomocysteinemia on cardiovascular risk factors and initiation of atherosclerosis in Wistar rats. Eur J Pharmacol. 2007; 574(1): 49–60, doi: 10.1016/j.ejphar.2007.07.022, indexed in Pubmed: 17706635.
27. Kirac D, Negis Y, Ozer NK. Vitamin E attenuates homocysteine and cholesterol induced damage in rat aorta. Cardiovasc Pathol. 2013; 22(6): 465–472, doi: 10.1016/j.carpath.2013.03.007, indexed in Pubmed: 23643071.
28. Bellamy MF, McDowell IF, Ramsey MW, et al. Hyperhomocysteinemia after an oral methionine load acutely impairs endothelial function in healthy adults. Circulation. 1998; 98(18): 1848–1852, doi: 10.1161/01.cir.98.18.1848, indexed in Pubmed: 9799203.
29. Charpiot P, Bescond A, Augier T, et al. Hyperhomocysteinemia induces elastolysis in minipig arteries: structural consequences, arterial site specificity and effect of captopril-hydrochlorothiazide. Matrix Biol. 1998; 17(8-9): 559–574, doi: 10.1016/s0945-053x(98)90108-1, indexed in Pubmed: 9923650.
30. Hidiroglou N, Gilani GS, Long L, et al. The influence of dietary vitamin E, fat, and methionine on blood cholesterol profile, homocysteine levels, and oxidizability of low density lipoprotein in the gerbil. J Nutr Biochem. 2004; 15(12): 730–740, doi: 10.1016/j.jnutbio.2004.04.009, indexed in Pubmed: 15607646.
31. Raaf L, Noll C, Cherifi ME, et al. Myocardial fibrosis and TGFB expression in hyperhomocysteinemic rats. Mol Cell Biochem. 2011; 347(1-2): 63–70, doi: 10.1007/s11010-010-0612-5, indexed in Pubmed: 20938722.
32. Ghoul A, Moudilou E, Cherifi ME, et al. The role of homocysteine in seminal vesicles remodeling in rat. Folia Histochem Cytobiol. 2017; 55(2): 62–73, doi: 10.5603/FHC.a2017.0010, indexed in Pubmed: 28636071.
33. Zhou J, Møller J, Danielsen CC, et al. Dietary supplementation with methionine and homocysteine promotes early atherosclerosis but not plaque rupture in ApoE-deficient mice.

Arterioscler Thromb Vasc Biol. 2001; 21(9): 1470–1476, doi: 10.1161/hq0901.096582, indexed in Pubmed: 11557674.
34. Liao D, Tan H, Hui R, et al. Hyperhomocysteinemia decreases circulating high-density lipoprotein by inhibiting apolipoprotein A-I Protein synthesis and enhancing HDL cholesterol clearance. Circ Res. 2006; 99(6): 598–606, doi: 10.1161/01.RES.0000242559.42077.22, indexed in Pubmed: 16931800.
35. Aasvee K, Jauhiainen M, Kurvinen E, et al. Determinants of risk factors of atherosclerosis in the postinfarction period: the Tallinn MI study. Scand J Clin Lab Invest. 2006; 66(3): 191–199, doi: 10.1080/00365510600564881, indexed in Pubmed: 16714248.
36. Au-Yeung KKW, Woo CWH, Sung FL, et al. Hyperhomocysteinemia activates nuclear factor-kappaB in endothelial cells via oxidative stress. Circ Res. 2004; 94(1): 28–36, doi: 10.1161/01.RES.0000108264.67601.2C, indexed in Pubmed: 14630727.
37. Lazzerini PE, Capecchi PL, Selvi E, et al. Hyperhomocysteinemia, inflammation and autoimmunity. Autoimmun Rev. 2007; 6(7): 503–509, doi: 10.1016/j.autrev.2007.03.008, indexed in Pubmed: 17643940.
38. Joseph J, Washington A, Joseph L, et al. Hyperhomocysteinemia leads to adverse cardiac remodeling in hypertensive rats. Am J Physiol Heart Circ Physiol. 2002; 283(6): H2567–H2574, doi: 10.1152/ajpheart.00475.2002, indexed in Pubmed: 12388235.
39. Matté C, Stefanello FM, Mackedanz V, et al. Homocysteine induces oxidative stress, inflammatory infiltration, fibrosis and reduces glycogen/glycoprotein content in liver of rats. Int J Dev Neurosci. 2009; 27(4): 337–344, doi: 10.1016/j.ijdevneu.2009.03.005, indexed in Pubmed: 19460627.
40. Devi S, Kennedy RH, Joseph L, et al. Effect of long-term hyperhomocysteinemia on myocardial structure and function in hypertensive rats. Cardiovasc Pathol. 2006; 15(2): 75–82, doi: 10.1016/j.carpath.2005.11.001, indexed in Pubmed: 16533695.
41. Othmani Mecif K, Aouichat Bouguerra S, Benazzoug Y. Plasma and aorta biochemistry and mmps activities in female rabbit fed methionine enriched diet and their offspring. J Nutr Metab. 2017; 2017: 2785142, doi: 10.1155/2017/2785142, indexed in Pubmed: 28133545.
42. Balcioğlu AS, Durakoğugil ME, Çiçek D, et al. Epicardial adipose tissue thickness and plasma homocysteine in patients with metabolic syndrome and normal coronary arteries. Diabetol Metab Syndr. 2014; 6: 62, doi: 10.1186/1758-5996-6-62, indexed in Pubmed: 24872849.
43. Wang G, Woo CWH, Sung FL, et al. Increased monocyte adhesion to aortic endothelium in rats with hyperhomocysteinemia: role of chemokine and adhesion molecules. Arterioscler Thromb Vasc Biol. 2002; 22(11): 1777–1783, doi: 10.1161/01.atv.0000035404.18281.37, indexed in Pubmed: 12426204.
44. Zhang R, Ma J, Xia M, et al. Mild hyperhomocysteinemia induced by feeding rats diets rich in methionine or deficient in folate promotes early atherosclerotic inflammatory processes. J Nutr. 2004; 134(4): 825–830, doi: 10.1093/jn/134.4.825, indexed in Pubmed: 15051832.
45. Dayal S, Wilson KM, Leo L, et al. Enhanced susceptibility to arterial thrombosis in a murine model of hyperhomocysteinemia. Blood. 2006; 108(7): 2237–2243, doi: 10.1182/blood-2006-02-005991, indexed in Pubmed: 16804115.
46. Postea O, Krotz F, Henger A, et al. Stereospecific and redox-sensitive increase in monocyte adhesion to endothelial cells by homocysteine. Arterioscler Thromb Vasc Biol. 2006; 26(3): 508–513, doi: 10.1161/01.ATV.0000201039.21705.dc, indexed in Pubmed: 16373615.
47. Charpiot P, Bescond A, Augier T, et al. Medial elastic structure alterations in atherosclerotic arteries in minipigs: plaque proximity and arterial site specificity. Matrix Biol. 1997; 15(7): 455–467, doi: 10.1016/s0945-053x(97)90019-6, indexed in Pubmed: 9106157.
48. Chaussalet M, Lamy E, Foucault-Bertaud A, et al. Homocysteine modulates the proteolytic potential of human vascular endothelial cells. Biochem Biophys Res Commun. 2004; 316(1): 170–176, doi: 10.1016/j.bbrc.2004.02.027, indexed in Pubmed: 15003526.
49. Bennett MR, Sinha S, Owens GK. Vascular smooth muscle cells in atherosclerosis. Circ Res. 2016; 118(4): 692–702, doi: 10.1161/CIRCRESAHA.115.306361, indexed in Pubmed: 26892967.
50. Tyagi SC. Homocysteine redox receptor and regulation of extracellular matrix components in vascular cells. Am J Physiol. 1998; 274(2): C396–C405, doi: 10.1152/ajpcell.1998.274.2.C396, indexed in Pubmed: 9486129.
51. Tsai JC, Wang H, Perrella MA, et al. Induction of cyclin A gene expression by homocysteine in vascular smooth muscle cells. J Clin Invest. 1996; 97(1): 146–153, doi: 10.1172/JCI118383, indexed in Pubmed: 8550827.
52. Murthy SN, Obregon DF, Chattergoon NN, et al. Rosiglitazone reduces serum homocysteine levels, smooth muscle proliferation, and intimal hyperplasia in Sprague-Dawley rats fed a high methionine diet. Metabolism. 2005; 54(5): 645–652, doi: 10.1016/j.metabol.2004.12.008, indexed in Pubmed: 15877295.
53. Yao D, Sun NL. Hyperhomocysteinemia accelerates collagen accumulation in the adventitia of balloon-injured rat carotid arteries via angiotensin II type 1 receptor. Int J Mol Sci. 2014; 15(11): 19487–19498, doi: 10.3390/ijms151119487, indexed in Pubmed: 25350112.
54. Liu Z, Luo H, Zhang Lu, et al. Hyperhomocysteinemia exaggerates adventitial inflammation and angiotensin II-induced abdominal aortic aneurysm in mice. Circ Res. 2012; 111(10): 1261–1273, doi: 10.1161/CIRCRESAHA.112.270520, indexed in Pubmed: 22912384.
55. Škovierová H, Vidomanová E, Mahmood S, et al. The molecular and cellular effect of homocysteine metabolism imbalance on human health. Int J Mol Sci. 2016; 17(10), doi: 10.3390/ijms17101733, indexed in Pubmed: 27775595.
56. Dai Y, Zhu J, Meng Di, et al. Association of homocysteine level with biopsy-proven non-alcoholic fatty liver disease: a meta-analysis. J Clin Biochem Nutr. 2016; 58(1): 76–83, doi: 10.3164/jcbn.15-54, indexed in Pubmed: 26798201.
57. Ai Y, Sun Z, Peng C, et al. Homocysteine induces hepatic steatosis involving ER stress response in high methionine diet-fed mice. Nutrients. 2017; 9(4), doi: 10.3390/nu9040346, indexed in Pubmed: 28368295.
58. Robert K, Chassé JF, Santiard-Baron D, et al. Altered gene expression in liver from a murine model of hyperhomocysteinemia. J Biol Chem. 2003; 278(34): 31504–31511, doi: 10.1074/jbc.M213036200, indexed in Pubmed: 12799373.
59. Luo X, Xiao L, Yang H, et al. Homocysteine downregulates gene expression of heme oxygenase-1 in hepatocytes. Nutr Metab (Lond). 2014; 11(1): 55, doi: 10.1186/1743-7075-11-55, indexed in Pubmed: 25520741.
60. Lynch SM, Strain JJ. Increased hepatic lipid peroxidation with methionine toxicity in the rat. Free Radic Res Commun. 1989; 5(4-5): 221–226, doi: 10.3109/10715768909074704, indexed in Pubmed: 2707623.
61. Mori N, Hirayama K. Long-term consumption of a methionine-supplemented diet increases iron and lipid peroxide levels in rat liver. J Nutr. 2000; 130(9): 2349–2355, doi: 10.1093/jn/130.9.2349, indexed in Pubmed: 10958834.

62. Tamanna N, Kroeker K, Braun K, et al. The effect of short-term methionine restriction on glutathione synthetic capacity and antioxidant responses at the whole tissue and mitochondrial level in the rat liver. Exp Gerontol. 2019; 127: 110712, doi: 10.1016/j.exger.2019.110712, indexed in Pubmed: 31472257.

Submitted: 27 July, 2021
Accepted after reviews: 18 May, 2022
Available as AoP: 30 May, 2022